

CONFERENCES AND SYMPOSIA PACS numbers: **06.20.–f**, 84.40.lk, 95.55.Sh

ON THE 100th ANNIVERSARY OF THE BIRTH OF N G BASOV

N G Basov's legacy: from the first masers to optical frequency standards

A A Belyaev, V G Voronzov, N A Demidov, K Yu Khabarova, N N Kolachevsky

DOI: https://doi.org/10.3367/UFNe.2022.11.039347

Contents

Abstract. The pioneering ideas of N G Basov, the centennial of whose birth was solemnly celebrated in 2022, laid the foundation for a number of modern research and technology areas in the field of quantum electronics and laser physics: from precision laser experiments aimed at testing the fundamental laws of physics to laser ignition of thermonuclear targets, from high-speed data transmission lines to laser welding and material processing. In this review paper, which was presented at the Basov centennial Scientific Session of the Physical Division of the Russian Academy of Sciences, we discuss the development and current state of the 'firstborn' of a series of scientific victories — the hydrogen maser (H-maser). The performance of H-masers is continuously being improved, and they are involved in solving a wide range of problems: time and frequency metrology, satellite navigation, and space radio astronomy. Russia is the recognized world leader in the development of maser technology, which is a brilliant example of the successful implementation of Basov's ideas. The natural development of this field is the advent of optical frequency standards, whose development prospects are discussed in the final part of the review.

Keywords: frequency standard, maser, H-maser, relativistic tests, VLBI, optical clocks

A A Belyaev (1), **V G Voronzov** (1), **N A Demidov** (1), **K Yu Khabarova** (2), **N N Kolachevsky** (2,*)
(1) JSC VREMYA-CH, ul. Osharskaya 67, 603105 Nizhny Novgorod, Russian Federation
(2) Lebedev Physical Institute, Russian Academy of Sciences, Leninskii prosp. 53, 119991 Moscow, Russian Federation
E-mail: (*) kolachevsky@lebedev.ru

Received 6 April 2023
Uspekhi Fizicheskikh Nauk **193** (10) 1091 – 1102 (2023)
Translated by E N Ragozin

1. Introduction

The principle of maser-laser oscillation formulated by N G Basov together with A M Prokhorov in long-ago 1952 [1] laid the basis of the functioning of a variety of devices that we use everywhere today, both in everyday life and in industry and scientific research. The future Nobel laureates predicted that an ensemble of identical molecular systems placed inside a volume resonator, in which the condition of population inversion is realized, will radiate narrow-band coherent radiation corresponding to the transition frequency. In this case, the spectral line width of this radiation should be much narrower than the width of the transition itself, by analogy with a resonant self-excited oscillator [2]. This idea formed the basis of N G Basov's doctoral dissertation, ''Molecular oscillator,'' which he defended at the age of 35. It is interesting to note that the question of the expected width of the line of such radiation caused a lot of disputes in the scientific environment around Basov: it was difficult to believe that the oscillator was supposed to radiate an actually unlimited narrow spectral line, and not a line corresponding to the spectral width of the transition. This was one of the reasons why, in addition to the former scientific supervisor (A M Prokhorov), such luminaries of science as V L Ginzburg, E K Zavoisky, V V Migulin, L A Artsimovich, and I M Frank gave feedback on the work, and A N Oraevsky described the defense of the dissertation as ''dramatic.''

By 1954, N G Basov also carried out the practical implementation of his idea: an experimental model of a molecular oscillator based on ammonia molecules was made in the USSR. Similar research was underway in the USA: C Townes, J Gordon, and H Zeiger made an ammonia oscillator at Columbia University in 1953. Hence, the well-established name of this device: maser (the acronym for microwave amplification by stimulated emission of radiation). As we know, for the fundamental contribution to the development of quantum electronics, which led to the advent

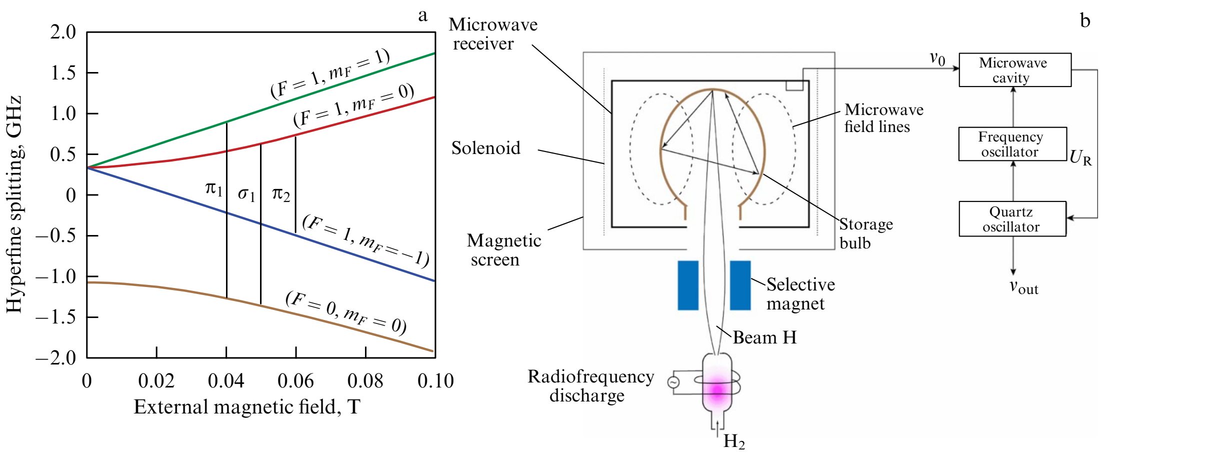

Figure 1. (a) Diagram of the ground state levels of a hydrogen atom in a magnetic field. (b) Schematic of a hydrogen maser.

of oscillators and amplifiers on the maser-laser principle, N G Basov, A M Prokhorov, and C Towns were awarded the Nobel Prize in 1964.

Like all ingenious inventions, the structure of the first ammonia maser operating at a frequency of 24 GHz turned out to be reasonably simple. A beam of gaseous ammonia passed through a selector of states, which provided the condition of population inversion, and entered the resonator, which formed the condition for stimulated emission. However, due to a number of reasons, the ammonia maser did not enjoy wide use in research and was replaced by its 'elder brother' — the hydrogen maser (H-maser). The hydrogen maser, operating on the hyperfine transition of the ground state of a hydrogen atom (Fig. 1) at a frequency of 1.42 GHz, was first proposed by Norman Ramsey in 1960 [3]. It turned out that among devices of this type it is the hydrogen maser that is best suited for developing frequency standards, including due to the unprecedented stability of the frequency of the output signal. For his developments in the field of precision spectroscopy and the development of the hydrogen maser [4], N Ramsey was awarded the Nobel Prize in 1989.

In the USSR, the development of the H-maser commenced in 1961 under the supervision of N G Basov, who immediately realized the wide potential of its practical use. It was clear that, in order to achieve high metrological characteristics, it was necessary to solve many scientific, technical, and technological problems: to ensure a high-quality selection of states, reduce losses, select the coating material of the bulb, suppress magnetic field fluctuations and cavity drifts, make high-quality electronics, and many more. V M Tatarenkov, a student and colleague of N G Basov's, headed this sphere and in 1966 moved from the Lebedev Physical Institute (LPI) to the All-Russian Scientific Research Institute of Physical, Technical and Radio Measurements (VNIIFTRI), where a group was set up to develop new frequency standards for that time. More recently, the technologies for making H-masers were transferred for production in Nizhny Novgorod, to the Nizhny Novgorod Scientific Research Instrument-Making Institute, Quartz, named after A P Gorshkov (NNIPI). Today, the world's best hydrogen masers are being developed and manufactured by the Russian company Vremya-Ch JSC (Nizhny Novgorod), which has sold several hundred of these complex devices throughout the world — about half of what has been produced in the world over recent decades. This is one of the successful and, unfortunately, infrequent examples of when the scientific leadership laid down by Soviet scientists was not only successfully implemented in technology but also demonstrated significant success on the world market.

There have been a number of variants of H-masers: active, passive, with sapphire resonators; continuous scientific and technical work is underway to improve their characteristics, reduce dimensions, and increase reliability. The relative instability of the H-maser frequency has reached 1×10^{-16} today, which actually coincides with the instability of the best primary fountain-type Cs standards. One may wonder why masers are not used as a primary standard, because then it would be possible to 'kill two birds with one stone' by simplifying the design of the primary standard and moving on to the cherished dream of all metrology physicists — to express the SI second in terms of fundamental constants. To do this, we can use the expression for the hyperfine splitting energy of the 1S state in the hydrogen atom

$$\Delta E_{\mathrm{HFS}} = \frac{8}{3}\,\mathrm{Ry}\,\alpha^2\,\frac{m_{\mathrm{e}}}{m_{\mathrm{p}}}\,g_{\mathrm{p}}$$

with the necessary corrections (relativistic, quantum electrodynamic, etc.). Here, Ry is the Rydberg energy, α is the fine structure constant, $m_{\mathrm{e}}/m_{\mathrm{p}}$ is the electron to proton mass ratio, and g_{p} is the proton g factor. With this approach, the second would be directly related to atomic energy units. However, this approach runs into two problems. On the one hand, the maser radiation frequency, despite its high stability, has a poor reproducibility. Due to the specific interaction of hydrogen atoms with the material of the inner surface of the storage bulb (usually teflon), the oscillation frequency of different H-masers can differ significantly (up to 10^{-12}), and the maser frequency is subject to a slow drift. Recall that the experimental accuracy of determining the frequency of the hyperfine transition in the hydrogen atom is 1420.405751767(1) MHz (relative accuracy: 7×10^{-13}) [5]. At the same time, the frequency reproducibility of modern fountain-type primary cesium standards is about 10^{-16} [6]. Another limitation is the theoretical accuracy of the $\Delta E_{\mathrm{HFS}}^{(\mathrm{theor})}$ calculation, which is at the level of 10^{-8} [7]. The error is associated primarily with the inaccuracy in determining the charge and magnetic radii of the proton. Therefore, H-masers, despite their apparent attractiveness, cannot be used as high-precision frequency standards with good reproducibility. Furthermore, due to the extremely high stability of the output signal frequency, they have gained

Table.

Parameter / Name	Optical frequency standards	Primary frequency standard	Commercial atomic beam clock	Compact atomic clock	Miniature atomic clock	Precision quartz clock	Quartz wrist watch
Error	10^{-18}	10^{-16}	10^{-13}	10^{-11}	10^{-10}	10^{-7}	10^{-5}
Instability	0.1 ns yr^{-1}	10 ns yr^{-1}	10 μs yr^{-1}	0.1 μs day^{-1}	1 μs day^{-1}	100 μs day^{-1}	1 s day^{-1}
Size	10^7 cm^3	10^7 cm^3	10^4 cm^3	100 cm^3	10 cm^3	1 – 10 cm^3	10 mm^3
Power	1 kW	1 kW	0.1 – 0.5 kW	1 W	120 mW	100 mW	10 μW
Price	> $5 mln	> $1 mln	$50,000	$2000	$300	$100	$1

wide application in metrology laboratories, playing the role of a frequency and time keeper (a kind of flywheel-integrator). H-masers are also widely used in terrestrial and space navigation, very long baseline radio interferometry (VLBI), and solving fundamental problems.

In addition to artificial masers, there are also natural cosmic objects that emit maser radiation. Specifically, the first cosmic maser based on the OH molecule (lasing wavelength: 18 cm) was discovered in 1965 [8]. One of the first reviews on cosmic masers was presented in the *Usp. Fiz. Nauk* (*Sov. Physics–Uspekhi*) journal in 1975 [9]. The most common cosmic maser sources are clusters of hydroxyl (OH), water (H_2O), methanol (CH_3OH), and silicon monoxide (SiO) molecules, which are pumped by external cosmic radiation.

In addition to H-masers, many different frequency standards have been created in recent decades, some of which are listed in the table. The standards have significantly different characteristics (accuracy and stability of the reproduced frequency, dimensions, power consumption, cost) and find application in various fields of science and technology where appropriate characteristics are required.

Back in distant 1968, N G Basov, together with V S Letokhov [10], pointed out the promise of optical frequency standards. The enormous path traveled by the scientific community over the past years has brought optical frequency standards to the level of a relative error of 10^{-19} [11], which confirms N G Basov's wildest expectations. The widespread practical demand for such precise standards is not yet obvious today, although they are successfully used in a variety of fundamental tests [12]. Today, the most apparent application for optical clocks with a relative error below 10^{-17} is gravimetry, since they are sensitive enough to measure the difference in gravitational potentials near the terrestrial surface (the relative frequency shift is about 10^{-16} m^{-1}). At the conclusion of the review, we discuss promising avenues for the development of optical clocks to improve their accuracy and reliability of operation.

2. H-masers in laboratories and space research

2.1 H-masers for state time services and scientific laboratories

The extremely high frequency stability and longevity of H-masers make them indispensable tools for national time services. While primary frequency standards (cesium beam standards and atomic fountains) provide reproduction of the SI second, masers, in turn, perform the function of a time keeper by integrating the signal over intervals from seconds to tens of days or more. A characteristic view of the Allan deviation of one of the best active H-masers manufactured in Russia (Ch1-1035, Vremya-Ch JSC) is shown in Fig. 2. One can see that the instability of the H-maser frequency decreases for measurement time intervals of more than 10^3 s and is less than 1×10^{-15}, reaching $(2-3) \times 10^{-16}$ for measurement time intervals of 10^5 s. Such an impressive result was achieved due to significant improvements to the system: additional stabilization of the resonator, mixing $m_F = -1$

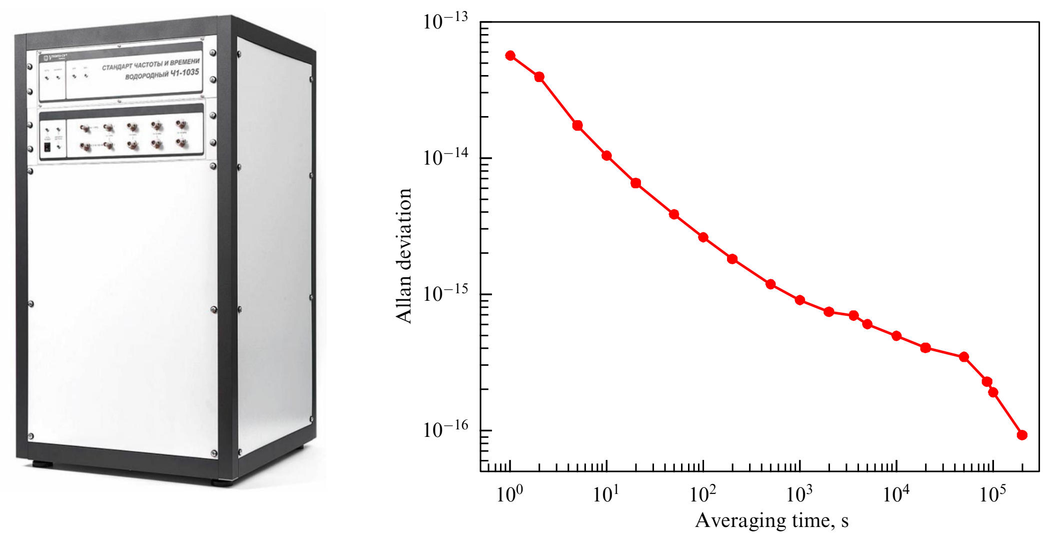

Figure 2. Allan deviation of the active H-maser Ch1-1035 manufactured by Vremya-Ch JSC.

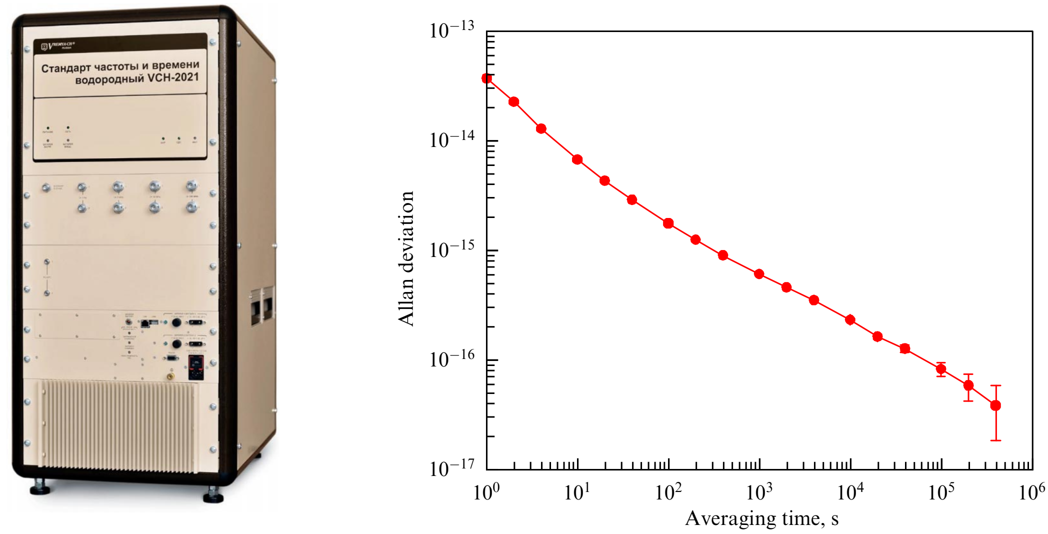

Figure 3. Allan deviation of the active H-maser VCH-2021 manufactured by Vremya-Ch JSC.

and $m_F = +1$ magnetic sublevels after the selector magnet, and a precision system for automatic resonator tuning [13].

To form a reliable time scale, large national metrology laboratories set up a complex of several H-masers, primary standards, and systems for mutual comparison and comparison with signals from global navigation satellite systems (GNSSs). Several H-masers operating simultaneously (usually in blocks of four) are required to increase system reliability. Frequency calibration in a continuous mode takes place using precision comparators and time interval counters, for example, Ch7-315.

Today, the National Metrological Institute of Russia (VNIIFTRI) operates the GET1 time standard, which includes a primary cesium fountain-type frequency standard, two rubidium fountain-type standards, 16 H-masers [14], and an optical frequency standard based on strontium atoms [15]. Due to the improvement in the reference base, including a significant improvement in the characteristics of H-masers, Russia's contribution to the formation of the global UTC time scale, which is formed by the BIMP service based on statistically weighted contributions from world frequency standards, has increased significantly. Today, the contribution of the Russian national scale UTC(SU) to UTC world time amounts to 17%. In turn, the contribution of hydrogen masers to the formation of the global time scale is greater than 90%.

Active and passive H-masers are also widely used in scientific laboratories where it is necessary to create a local 'institutional' frequency and time scale. Calibration of an active H-maser frequency using GNSS signals allows, after long averaging (about 10 days), generating a reference frequency signal with a relative reproduction accuracy of 10^{-15}, which is limited by the capabilities of the comparison channel with the satellite signal. Such a local scale is in demand both for precise radio frequency measurements and calibrations, and for precision spectroscopy tasks in the optical range [16].

Improving H-masers further involves the use of technology for obtaining a beam of hydrogen atoms in one quantum state (atoms in the state with $F = 1$, $m_F = -1$ atoms are excluded from the beam), which makes it possible to reduce the contribution of thermal noise of the resonator to frequency instability by approximately 1.5 times. This technology was introduced into the promising hydrogen frequency and time standard VCH-2021 (Fig. 3), which made it possible to achieve frequency instability of less than 1×10^{-16} over a measurement time interval of 1 day. At the moment, preparations are underway for main production of VCH-2021 [17].

Passive hydrogen frequency standards are significantly smaller in size, mass, and price. In terms of immunity to and strength against external influences, the passive hydrogen frequency standard is significantly superior to active hydrogen standards and has an order of magnitude higher performance than rubidium and cesium frequency standards. The external view and Allan deviation of the industrially produced passive hydrogen frequency standard VCH-1008M are presented in Fig. 4.

When introducing double atomic sorting technology into passive frequency standards, it is possible to reduce the frequency instability over a measurement time interval of 1 day down to 5×10^{-16}. In this case, the physical part of the device (hydrogen discriminator) will lengthen by about 60 mm.

2.2 H-masers in tests of fundamental theories and space missions

In his pioneering work of 1961, "On the possibility of studying relativistic effects using molecular and atomic frequency standards" [18], N G Basov proposed the use of the unique properties of maser radiation in tests of the General and Special Theory of Relativity (GTR, STR), as well as the study of cosmological effects. The surprising thing is that just half a century ago the canonical higher-order GTR correction responsible for the frequency shift in the gravitational field, $\Delta f / f = \Delta U / c^2$, continued to cause controversy and discussion (ΔU is the difference among gravitational potentials at observation points). The correction is called gravitational redshift, since the frequency of radiation decreases with decreasing gravitational potential (when moving away from a massive object).

An example is provided by the launch of the first satellites of the American GPS system in 1977. GTR predicts that the course of clocks in orbit should differ from their course on

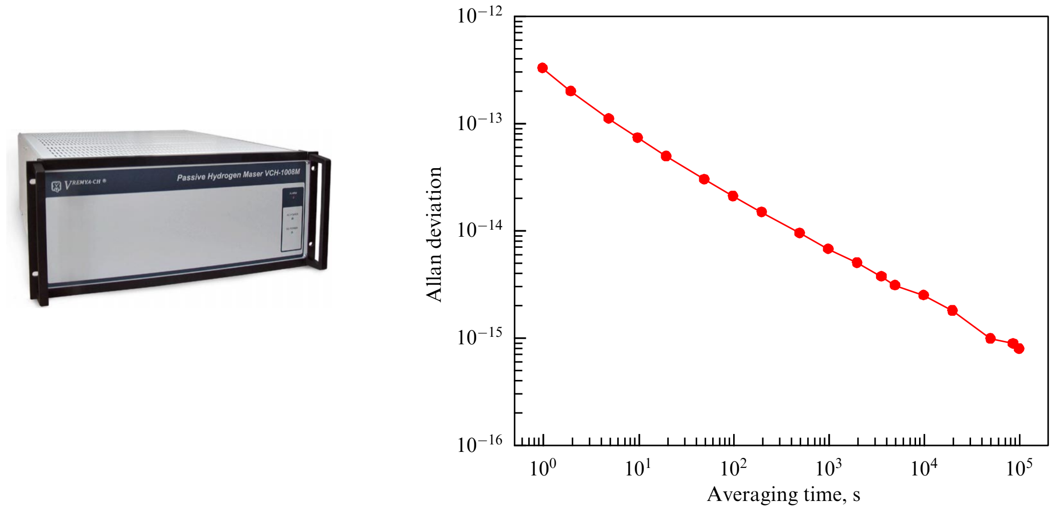

Figure 4. Allan deviation of the passive H-maser VCH-1008M manufactured by Vremya-Ch JSC.

Earth due to two effects: gravitational displacement and time dilatation. For the GPS satellite orbit (20,000 km), the relative correction when the signal arrives at Earth's surface is about $+5 \times 10^{-10}$, and its inclusion is absolutely critical for providing navigation accuracy [19, 20]. However, the satellite designers were not sure not only of the magnitude of this correction but even of its sign, so the capacity to adjust the frequency of the transmitted signal was introduced. After three weeks of comparison with ground stations, the correction was calculated experimentally (4.425×10^{-10}), which coincided with the theoretical prediction with an accuracy of 1% [19].

For a detailed study of the contribution of general relativity effects, American scientists carried out the Gravity Probe A (GPA) mission at approximately the same time (1976). An active H-maser was installed on a rocket launched into a suborbital flight to an altitude of 10,000 km, whose frequency was compared with the ground standard throughout the entire flight. As a result of the experiment, it was found that the possible deviation from the prediction of the theory $\Delta f/f = (1+\alpha)\Delta U/c^2$ (here, α is a measure of deviation) does not exceed $|\alpha| < 7 \times 10^{-5}$ [21]. This result remained a record for sensitivity until recently (2018), when the limitation was strengthened fivefold by analyzing signals from the GALILEO satellites located in a slightly eccentric orbit [22].

The next launch of an active H-maser into space after GPA took place in 2011 as part of the Russian space mission Spektr-R (RadioAstron, Lebedev Physical Institute). The RadioAstron mission, brought into being by Academician N S Kardashev, is a radio interferometer with a very long base (VLBI), one of the arms of which is placed on a spacecraft orbiting Earth in an elliptical orbit [23]. By doing this, it was possible to significantly increase the interferometer base up to 300,000 km, which made the device the most sharp-sighted of the existing VLBI telescopes. When observing maser cosmic sources, an angular resolution of 8 μs of arc was achieved, which is today a world record.

In order to ensure that a signal is recorded by a space antenna for subsequent processing on a correlator (Fig. 5), there must be a frequency standard aboard the device that provides accurate time stamps. N S Kardashev decided to install aboard the spacecraft two active H-masers produced by Vremya-Ch JSC (VCH-1010 No. 004-07 and No. 005-07), which had sufficient characteristics to support the mission. This was a major risk, since the reliability of H-masers on long-duration space missions had not been studied.

After the radio telescope was launched and put into orbit, one of the on-board H-masers turned out to be faulty, but the second one was successfully launched and operated in orbit for about six years (the entire mission lasted from 2011 to 2018). The characteristics of the H-maser used aboard RadioAstron and measured before launch are presented in Fig. 6.

The RadioAstron Russian 21st century project made it possible to obtain unique data on quasars and active galactic nuclei, pulsars, and galactic and extragalactic sources of maser radiation. Data processing continues: scientists are analyzing the results accumulated during the period of RadioAstron's operation.

The next LPI project is the Spektr-M mission (Millimetron observatory) [24]. This is also a VLBI telescope, operating in the millimeter wavelength range (from 80 μm to 3 mm), which will allow advanced research into the physics of supermassive black holes, details of the origin of the Universe and the era of reionization to be revealed, research on the formation of stars and planets to be carried out, and searching for traces of water. To ensure the VLBI mode, as in the case of RadioAstron, an on-board frequency standard is required, for which an H-maser with improved characteristics is planned (Fig. 7). In this case, the lifespan of the devices is more than 10 years, the weight is no more than 56 kg, and the overall dimensions are $\varnothing$ 460 × 671 mm.

Therefore, Russia not only was the first in the world to launch an active H-maser into a long orbital flight but also significantly improved the characteristics of such on-board systems, which makes us an absolute world leader. This experience and developments have to continue advancing, taking into account the ambitious plans of teams from Europe [25], the USA, and China, which are actively working in this area.

2.3 H-masers in global satellite navigation systems

Improving the frequency stability of the on-board synchronizing device in GNSS systems remains an important task and remains relevant, despite significant progress in recent

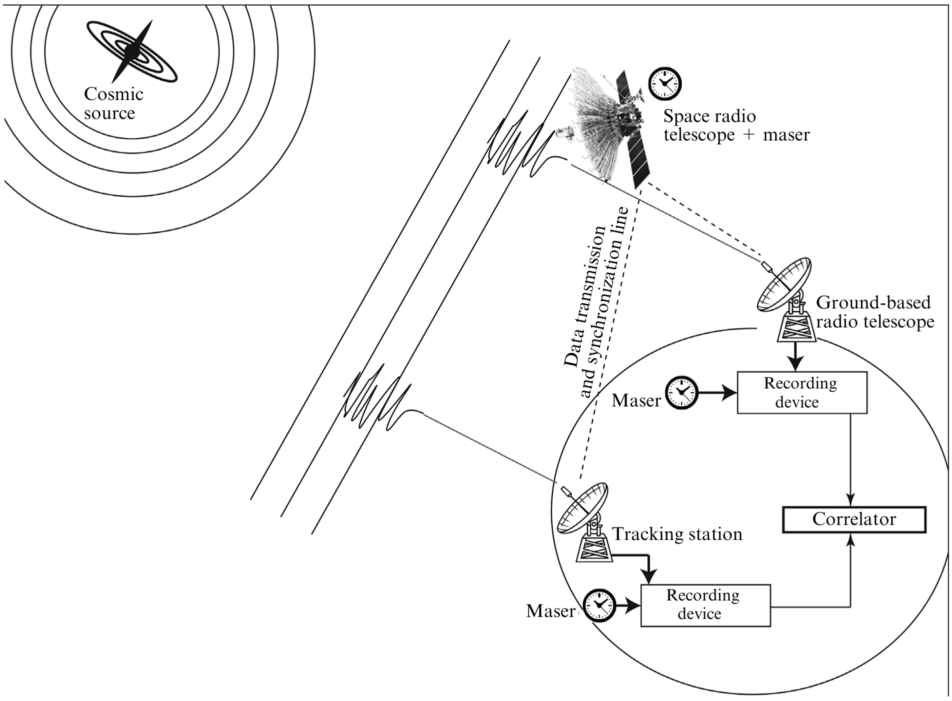

Figure 5. VLBI scheme. Signal received by the antenna is amplified, digitized, and recorded synchronously along with time stamps provided by the frequency standard. After this, signals from two (or more) antennas are applied to a correlator, where the signal is processed.

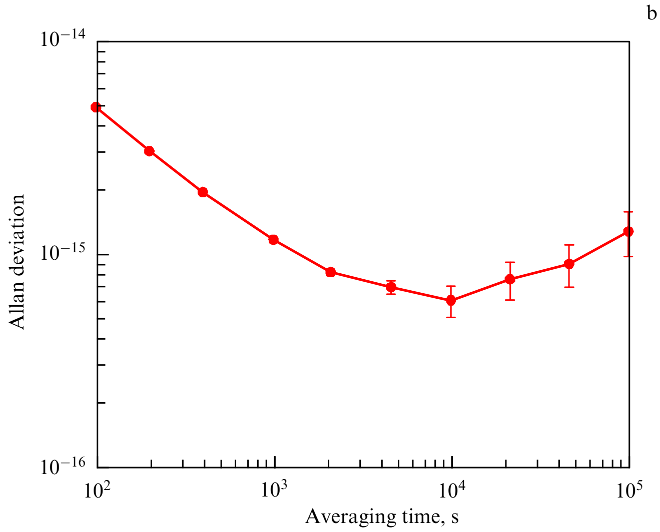

Figure 6. (a) Hydrogen maser installed aboard the RadioAstron space telescope. (b) Allan deviation of the maser frequency minus linear drift. To record data aboard, intervals of about 1000 s were used, which corresponds to a relative frequency error of 10^{-15}.

decades. Specifically, the daily signal instability of the Glonass-M and Glonass-K satellites is 1×10^{-13}, and for the Glonass-K2 satellite it is 5×10^{-14} [26]. Considering that the relative error of the on-board clock at the level of 1×10^{-14} or 1 ns day^{-1} corresponds to an error of 30 cm in determining the pseudo-range, we can conclude that the contribution of the error of existing on-board systems remains significant for the margin of error in determining the position. In existing GLONASS devices, the on-board synchronizing device includes a complex of a cesium beam clock and a rubidium cell clock. A decision was made on the need to reduce the error in the next generations of GLONASS devices to the level of 5×10^{-15} (1 day) and further to 2×10^{-15} (1 day) in prospective systems. At the same time, the potential of rubidium and cesium standards is virtually exhausted today.

In 2016, the European Union began populating its own GNSS orbital constellation, GALILEO. The principle of operation of GALILEO does not differ from the GPS and GLONASS that existed before it. However, the Europeans decided to install a passive H-maser as an on-board standard (instead of a cesium beam clock). When developing the design of this maser [27], the results obtained by scientists from Nizhny Novgorod were used. Despite the skepticism that arose at the beginning of the project regarding the reliability of the operation of H-masers on board, the measured characteristics clearly indicated that the instability of the frequency of passive H-masers is many times lower than the

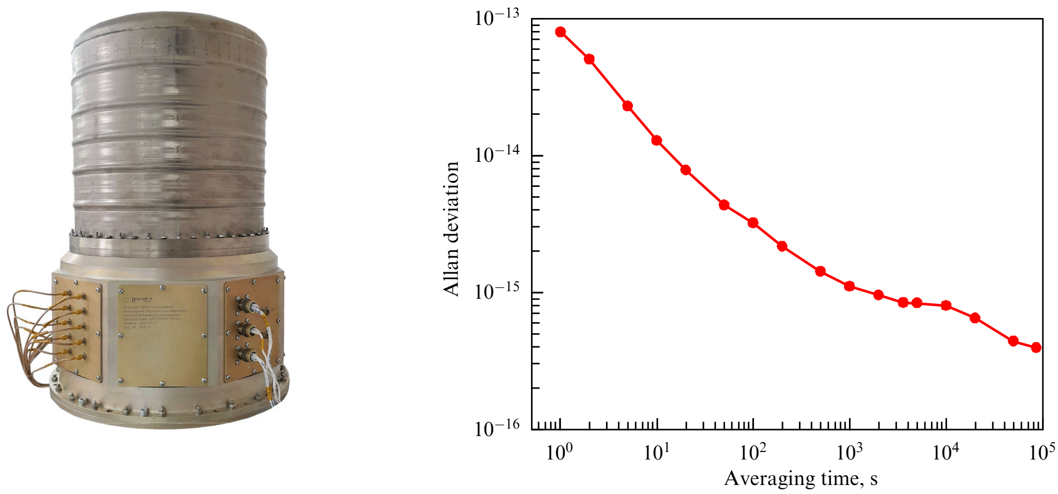

Figure 7. On-board H-maser from Vremya-Ch JSC for the Millimetron mission (LPI).

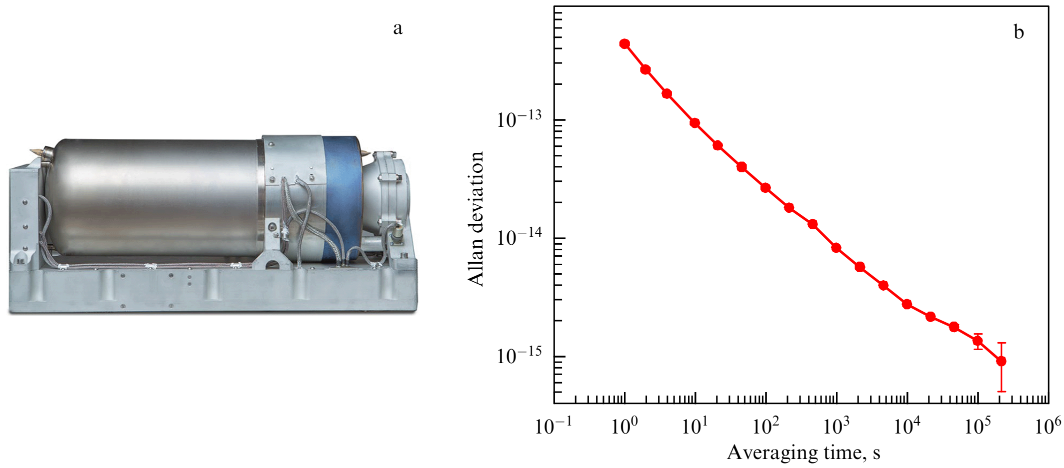

Figure 8. (a) Passive H-maser produced by Vremya-Ch JSC. (b) Characteristics of the output signal of the H-maser developed in Russia.

instability of on-board rubidium standards [28]. Specifically, the frequency instability is as low as 7×10^{-15} with a drift of only 1.9×10^{-14} day^{-1}. The installation of such a high-quality on-board frequency standard was one of the key reasons why the accuracy of position determination using GALILEO signals — less than 1 m in the normal mode — is several times higher than the accuracy provided by GPS and GLONASS systems.

As mentioned above, the design of a passive H-maser for space use was initially developed in Russia, and the first working samples were made approximately simultaneously with those of the Europeans (Fig. 8). At the same time, the characteristics of the latest samples of passive H-masers are in many ways superior to foreign ones, including those installed in the GALILEO system. Specifically, the frequency instability is as low as 1.5×10^{-15} over a measurement time interval of 1 day, with a device weight of 12.5 kg and overall dimensions of $470 \times 170 \times 200$ mm.

So, taking into account the characteristics of the output signal, the dimensions and reliability, a passive H-maser today seems to be the best opportunity for upgrading the on-board synchronization device on GLONASS satellites. Flight testing of the passive H-maser is scheduled for 2023, and we hope that it will demonstrate the required performance in operation with the system of on-board equipment. In the development of promising on-board systems, it is also planned to use optical frequency standards [29, 30], which are currently being developed in cooperation with Russian organizations (JSC RKS, Lebedev Physical Institute, and Skoltech).

3. Prospects for the development of optical frequency standards

3.1 Transition from the microwave to the optical region

The fundamental study by N G Basov, "Optical frequency standards" [10], written in collaboration with his student and colleague V S Letokhov, outlined the development path in the field for decades to come. Increasing the carrier frequency from the 10^{10}-Hz range (microwave range) to the $10^{14}-10^{15}$-Hz domain (optical range) provides a corresponding increase in the quality factor of atomic resonances Q. As a consequence, the accuracy and stability of frequency standards increases in accordance with the expression

$$\sigma_y(\tau) = \frac{1}{K}\frac{1}{Q}\frac{1}{\mathrm{S/N}}\frac{1}{\sqrt{\tau/c}}\,.$$

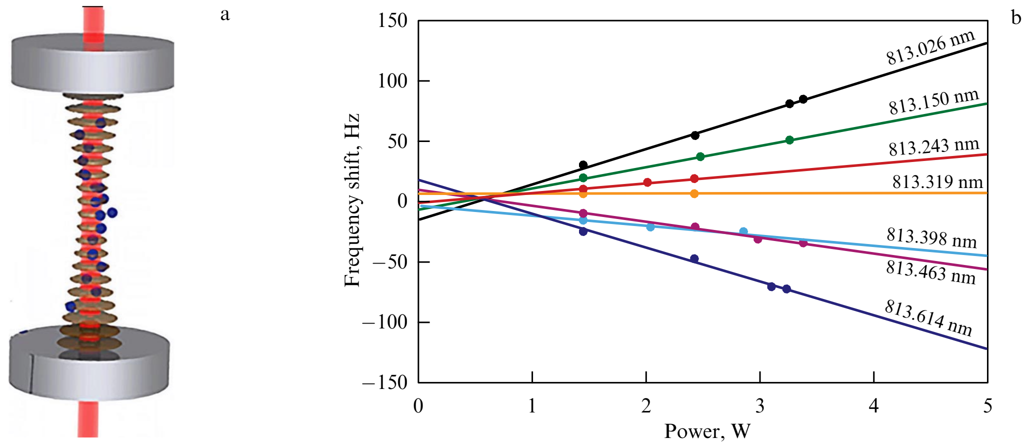

Figure 9. (a) Atoms in a vertical optical lattice formed by a standing wave in a Fabry–Perot cavity. (b) Experimental determination of the magic wavelength. Measurements are made of the shift of the line center and the line wavelength in relation to the power of the optical lattice.

Here, K is a coefficient of the order of unity, and S/N is the signal-to-noise ratio. Furthermore, a major advantage of optical standards is a significant, by several orders of magnitude, reduction in the averaging time to reach a given level of instability. While for microwave standards the time to reach the 10^{-16} level takes about 10 days, for optical systems this may require from 1 to 100 s (depending on the characteristics of the interrogating laser). This property opens up the possibility of rapid analysis of systematic effects that are present in the system and limit accuracy.

The era of optical frequency standards, which was opened up in the USSR by N G Basov and picked up by V S Letokhov (who in 1970 moved from LPI to ISAN (Institute of Spectroscopy of the Russian Academy of Sciences)), V P Chebotaev (Rzhanov Institute of Semiconductor Physics (ISP) SB RAS, since 1991 Institute of Laser Physics (ILP) SB RAS), and many other outstanding scientists of that time, has today seen a blossoming in this area. Experiments performed using optical clocks make it possible to implement the most sensitive tests of fundamental physical theories (search for the drift of the fine structure constant, search for dark matter, sensitive tests of the effects of special relativity and general relativity, tests of the equivalence principle), which is reflected in a number of reviews [12, 31]. Today, there are a number of optical frequency standards operating on both neutral atoms [32, 33] and ions [34, 35], for which the relative frequency reproducibility has crossed the 18th decimal place, which confirms the wildest expectations of N G Basov and his colleagues.

A partial review of work on single-ion clocks and development prospects is presented in Ref. [36]. Here, we briefly summarize the progress on the development of ultracold lanthanide optical clocks at LPI since 2016, when the use of thulium as a frequency standard was substantiated in Ref. [37]. Since the metrological (clock) transition in the thulium atom has not been studied by other groups, in the remainder of the review we will present the results of a typical cycle of research that accompanies the development and characterization of any optical standard based on neutral atoms.

3.2 1.14-μm magnetic dipole clock transition in thulium atoms

To implement a neutral-atom optical clock, first of all, it is necessary to cool the atomic ensemble to a temperature of 1–10 μK, which will provide the possibility of reloading an optical lattice formed by a standing light wave (Fig. 9).

Two-stage cooling of Tm atoms was first implemented at the LPI, which makes it possible to cool a cloud consisting of 10^6 atoms to a temperature of less than 25 μK [38]. The optical lattice performs two functions: (1) confinement of atoms to increase the interaction time with the interrogating laser radiation (up to several seconds) and (2) providing the Lamb–Dicke regime, in which the atom is localized in a region of space much smaller than the wavelength of the exciting light [39]. When the Lamb–Dicke condition is satisfied, the first-order Doppler effect does not affect the carrier frequency, and the corresponding frequency shift becomes zero.

However, the polarization of atoms, which ensures their retention in the lattice, is simultaneously responsible for a light frequency shift (dynamic Stark effect). A breakthrough proposal that has now found application in all neutral-atom clocks was the use of the so-called 'magic' wavelength, at which the difference polarizability of the upper and lower clock levels is zero to the first order (linear approximation) [39]. Usually, the position of the magic wavelength is first estimated by calculations and then defined more precisely in experiment. Finding and analyzing the magic wavelength is an independent research task.

For the clock magnetic dipole transition in thulium atoms, we calculated the difference polarizabilities of the clock levels and identified candidates for the magic wavelength in the vicinity of 808, 813, and 1063 nm [40]. Precise measurements for the 813-nm range showed that the polarizabilities of the upper and lower levels are equal for $\lambda_{m1} = 813.320$ nm (Fig. 9b).

This wavelength can be provided by a Ti:Sa laser or a semiconductor laser. Note that the quality of the signal read from the clock transition of atoms in an optical lattice depends significantly on the spectral properties of the lattice radiation — on the level of phase and amplitude noise. When tuned to the magic wavelength, the spectrum of the clock transition narrows (the power broadening disappears). In our experiments with thulium atoms, lines with a spectral width of about 10 Hz were usually used, which is limited by the duration of the exciting field pulse (80 ms). Further narrowing of the line when working in the optical clock mode is usually not advisable, since it significantly lengthens the experimental cycle and does not result in a decrease in σ_y.

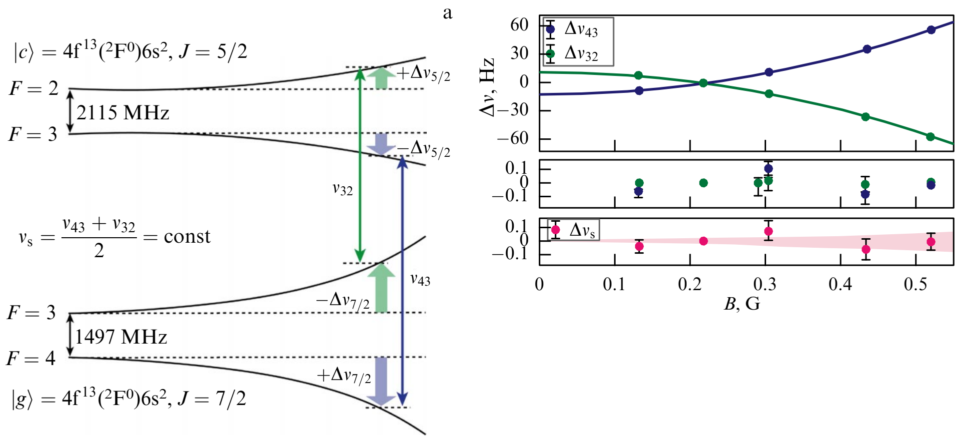

Figure 10. (a) Clock transition levels in thulium-169 atoms with inclusion of the hyperfine structure. Bichromatic laser field simultaneously interrogates two clock transitions, ν_{43} ($F = 4 \to F = 3$) and ν_{32} ($F = 3 \to F = 2$), in both cases Zeeman components with zero spin projection ((0–0) transitions). Synthetic frequency $\nu_S = (\nu_{43} + \nu_{32})/2$ is insensitive to the magnetic field. (b) Measurement of Zeeman shifts $\Delta\nu_{43}$ and $\Delta\nu_{32}$ in external magnetic field B for two clock transitions, ν_{43} and ν_{32}, respectively. Bottom graph shows the behavior of synthetic frequency ν_S.

In subsequent experiments, we plan to use a different magic wavelength, $\lambda_{m2} = 1063$ nm, due to a number of advantages: the availability of higher-power and more stable laser sources, a large detuning from nearby resonances, and a corresponding reduction in scattering. Therefore, from the point of view of the spectral width of the resonance, the number of atoms, and the characteristics of the optical lattice, thulium optical clocks are on a par with other common systems that use strontium [32] and ytterbium [41]. Note that optical clocks based on neutral Sr are considered by the metrological community to be the main candidate for redefining the SI second due to their widespread use in the world and successfully confirmed comparisons. Certain disadvantages of thulium clocks include a lower resonance frequency (1.6 times lower than in strontium) and a large Zeeman shift.

An extremely important characteristic of any optical clock is the contribution of systematic effects that must be controlled with high precision. A significant contribution to the margin of error of neutral-atom optical clocks usually comes from: (1) a shift by blackbody radiation; (2) a Zeeman shift; (3) higher-order shifts from the optical lattice, collisions, etc. [42]. For instance, in a strontium clock, the relative shift of the clock transition (698 nm) by blackbody radiation is -5500×10^{-18} (at room temperature 300 K). To achieve the 18th digit level, it is therefore necessary to control the contribution of this effect with extremely high precision or cool the facility to cryogenic temperatures [33].

We have experimentally shown that, due to the unique structure of levels in thulium and the specificity of the 1.14-μm magnetic dipole transition, the frequency shift under blackbody radiation, which is described by the expression

$$\Delta\nu_{\mathrm{BBR}} = -\Delta\alpha_0^{\mathrm{S}} \frac{\pi^2 a_0^3 k_{\mathrm{B}}^4}{15 c^3 \hbar^4} T^4 ,$$

turns out to be extremely low. Here, $\Delta\alpha_0^{\mathrm{S}}$ is the difference scalar polarizability (static) of the upper and lower clock levels, a_0 is the Bohr radius, k_{B} is the Boltzmann constant, and T is the ambient temperature. In Ref. [43], we experimentally determined the difference dynamic scalar and tensor polarizability in a broad spectral range for the 1.14-μm transition, which allowed us to determine that at room temperature the shift by black body radiation in thulium is only 2.3×10^{-18}, 2000 times lower than in optical clocks based on strontium atoms. This result significantly relaxes the temperature control requirements and permits the development of compact transportable systems [44].

A detailed study of another dominant systematic effect, the Zeeman shift, showed that it can be completely eliminated in the thulium atom by measuring the so-called 'synthetic' frequency, which is a combination of the frequencies of two transitions. The very idea of a synthetic frequency is not new [45]; however, at the LPI, it was possible for the first time to realize the simultaneous (rather than sequential) excitation of two clock transitions, which makes it possible to completely eliminate the influence of the magnetic field [46]. Figure 10 shows the system of levels of the 1.14-μm clock transition in the thulium-169 atom, with the inclusion of the hyperfine structure of the lower and upper levels.

Since the spin of the thulium atom nucleus is $I = 1/2$, the Breit–Rabi formula for level splitting in a magnetic field applies, which has the form

$$E_{F=J\pm1/2}(m_F, B) = E_F^0 + g_J \mu_{\mathrm{B}} B m_F \pm \frac{(g_J - g_I)^2 \mu_{\mathrm{B}}^2 B^2}{4E_{\mathrm{HFS}}} \left(1 - \frac{m_F^2}{(2J+1)^2}\right),$$

where B is the magnetic field strength, m_F is the magnetic quantum number, and J is the quantum number of the total moment of the electron shell of the atom. It is clear from the formula that the upper ($F = J + 1/2$) and lower ($F = J - 1/2$) components of the hyperfine structure for each electronic level shift in a magnetic field absolutely symmetrically, which ensures complete independence of the synthetic frequency $\nu_S = (\nu_{43} + \nu_{32})/2$, which is the half-sum of two frequencies, from the magnetic field B. Zeeman shift compensation has been studied experimentally (Fig. 10b), which confirms at least a 1000-fold Zeeman shift compensation.

An important feature of the studies performed was the simultaneous interrogation of two hyperfine components of clock transitions, which is technically relatively easy to implement using acousto-optical modulators. It is due to simultaneous interrogation that the contribution of magnetic field fluctuations, which is inevitable in a sequential scheme, is completely compensated. The experimental demonstration and verification of such a scheme open up new possibilities in the field of developing optical clocks with a minimal contribution of systematic effects. The difficult part of this task was controlling the population transfer between the four clock levels that occurs in the course of spontaneous decay of the upper levels. In the thulium atom, the transition interrogation time (several ten ms) is comparable to the lifetime of the upper level (130 ms), which may potentially lead to distortion of the spectra and frequency shifts. A thorough analysis of population transfer processes carried out in Ref. [46] showed that these shifts do not exceed 2×10^{-18}.

Measurements have demonstrated that the relative instability of the synthetic frequency does not exceed 10^{-16} for an averaging time of 1000 s, which is currently limited by the noise of the laser system and the capabilities of the measurement technique. Estimates of the relative instability made by comparing different subsets of experimental data and partial compensation of laser noise (comparing two clock transitions) suggest that the frequency dispersion of the clock transition amounts to 20 mHz (7×10^{-17} in relative units) [46]. In terms of statistical characteristics, thulium clocks are still far inferior to their main competitors — strontium and ytterbium clocks based on optical lattices. An improvement can be achieved through the use of a next generation interrogating laser, for example, stabilized to a cryogenic silicon resonator [47].

As noted above, a key characteristic of optical clocks is the magnitude of the systematic shifts. The thulium clock is one of the record holders among optical clocks based on neutral atoms, combining an extremely low contribution of the blackbody radiation shift and full compensation of the Zeeman shift. An analysis of all other known shifts performed in Ref. [43] suggested that their total contribution does not exceed 1.7×10^{-17} (without compensation, at room temperature), with the main contribution being made by the field of the confining optical lattice. This opens up strong opportunities for designing transportable systems that provide frequency accuracy and reproducibility at the level of one 17th digit, which is in wide demand in metrological support, navigation, and gravimetry tasks [48].

Our group has taken the first steps towards making a transportable thulium clock: a compact magneto-optical trap without a Zeeman decelerator has been designed and characterized [44], with attributes not inferior to those of the previous generation. Using the new setup, the first experiments on deep cooling of thulium atoms and capture into an optical lattice were performed. Currently, research is being carried out on deeper cooling of atoms (the third stage of cooling at a narrow 506-nm transition) to reduce the contribution of optical lattice shifts, and work is underway to define more precisely the magic wavelength in the vicinity of 1063 nm. The goal of the next experiments is to compare the two systems, demonstrate the relative instability at the 10^{-17} level, and conduct research on the influence of the gravitational potential on the thulium clock, which will be carried out by raising one of the systems relative to the other by several ten centimeters (similar to Refs [49, 50]).

Another important problem that needs to be solved in the development of next-generation optical clocks is eliminating the contribution of the Dick effect [51]. The Dick effect occurs in systems with periodic signal readout, with the result that some of the high-frequency noise of the interrogating laser is transferred to the low-frequency range and degrades the statistical characteristics of the optical clock. The contribution of the Dick effect to instability is described by the expression

$$\sigma^2_{\mathrm{Dick}}(\tau) = \frac{1}{\tau}\sum_{n=1}^{\infty}\left|\frac{G_n}{G_0}\right|^2 S_y\left(\frac{n}{T_{\mathrm{c}}}\right),$$

where T_{c} is the total atom interrogation period, $S_y(f)$ is the spectral noise density of the interrogating laser at frequency f, and $G(t)$ is a function describing the response of the atomic system to a small phase deviation of the interrogating laser. It can be seen that the σ_{Dick} contribution decreases according to the law $1/\sqrt{\tau}$ (quite slowly) and significantly worsens the clock characteristics for all averaging times. The Dick effect is actually a manifestation of the moiré effect, which, for example, is observed in digital oscilloscopes (with strictly periodic digitization of the input signal) when recording high-frequency signals at a slow-sweep time base.

The Dick effect can be reduced by using ultra-low noise interrogation lasers (for example, based on cryogenic resonators) [52] or by using two independent interrogation systems. For instance, in experiments with two strontium clocks [53], it was shown that synchronous interrogation makes it possible to reduce the relative instability of systems by approximately an order of magnitude (from 10^{-15} every 100 s to 10^{-16} every 100 s) by eliminating the Dick effect. However, this method is very time consuming and expensive. Reducing the intrinsic noise of an interrogating laser is a separate time-consuming task; today, silicon cryogenic resonators with instability below 10^{-16} (1 s) operate successfully only in the USA and Germany.

One way to eliminate the Dick effect is with a continuously operating optical clock. Such systems can either use atomic beams [54] or operate in laser or superradiant mode at a narrow metrological transition [55]. Our group has also considered the possibility of making a continuous-wave thulium optical clock, taking advantage of full Zeeman shift compensation at the synthetic frequency [56]. Unfortunately, fully operating continuous-type clocks have not yet been implemented, both due to significant technical difficulties and due to the increased contribution of a number of systematic effects in comparison with 'classical' optical clocks with periodic interrogation. There is some analogy with attempts to make continuous-type cesium atomic fountains for metrological support of national laboratories, which has not yet been implemented [57].

Therefore, using the example of designing a thulium optical lattice clock at the Lebedev Physical Institute, we showed the path of development of similar neutral-atom systems and identified certain scientific and technical challenges in the development of this area.

4. Conclusions

The development of frequency standards continues along two lines: for solving applied problems and for fundamental research. As it seems today, frequency standards that provide relative instability and reproducibility at the level of 10^{-16} 'cover' the basic needs of society in such widespread areas as navigation and telecommunications. Operating in this massive field are hydrogen masers of various types, atomic fountains, clocks based on beams and atomic cells, and quartz oscillators. The struggle continues to increase reliability and compactness and to reduce energy consumption, as well as to enter the space sector. So far, higher-precision systems are most widely used in fundamental research, and the most visible practice-oriented area is relativistic geodesy.

At the same time, progress in optical frequency standards has not stopped: in measurements of gravitational displacement in a millimeter cloud of cold atoms, which was carried out by a group of researchers from the USA in 2022, a relative error of 7.6×10^{-21} was achieved [58]. And this result crossed the limit $(10^{-15} - 10^{-20})$, which Nikolai Gennadievich Basov marked with a bold hand in chalk on a blackboard about 60 years ago, which is captured in one of the historical photographs published in honor of the 100th anniversary of his birth [59]. A search is underway for new transitions that are the least sensitive to external influences (multiply charged ions [60], nuclear standards [61, 62]), laser systems are being improved, compact femtosecond optical frequency combs are being developed for transition from the optical range to the radio frequency range [63], and more and more compact and reliable systems are being devised. Years will pass, and new, more accurate frequency standards will find wider application in various aspects of our lives (maybe some that we are not aware of today), and the characteristics of advanced developments will improve and open up new opportunities for comprehending the world.

References

1. Basov N G, Prokhorov A M, in *Vsesoyuz. Konf. po Radiospektroskopii, Mai 1952, AN SSSR* (All-Union Conf. on Radio Spectroscopy, May 1952, USSR Academy of Sciences)
2. Basov N G, Prokhorov A M *Usp. Fiz. Nauk* **57** 485 (1955)
3. Kleppner D, Goldenberg H M, Ramsey N F *Phys. Rev.* **126** 603 (1962)
4. Ramsey N F *Angew. Chem. Int. Engl. Ed.* **29** 725 (1990)
5. Hellwig H et al. *IEEE Trans. Instrum. Meas.* **19** 200 (1970)
6. Weyers S et al. *Metrologia* **55** 789 (2018)
7. Mohr P J, Taylor B N *Rev. Mod. Phys.* **77** 1 (2005)
8. Weaver H et al. *Nature* **208** 29 (1965)
9. Strel'nitskii V S *Sov. Phys. Usp.* **17** 507 (1975); *Usp. Fiz. Nauk* **113** 463 (1974)
10. Basov N G, Letokhov V S *Sov. Phys. Usp.* **11** 855 (1969); *Usp. Fiz. Nauk* **96** 585 (1968)
11. Brewer S M et al. *Phys. Rev. Lett.* **123** 033201 (2019)
12. Safronova M S et al. *Rev. Mod. Phys.* **90** 025008 (2018)
13. Vorontsov V G et al., in *Metrologiya Vremeni i Prostranstva. Mezhdunarodnyi Simpozium, Mendeleevo, Moskovskaya Oblast', Rossiya, 12–14 Sentyabrya 2018* (Metrology of Time and Space. Intern. Symp., Mendeleevo, Moscow Region, Russia, 12–14 September 2018) (Exec. Ed. L A Tokina) (Mendeleevo: VNIIFTRI, 2018)
14. Table 4. Equipment and source of UTC(k) of the laboratories contributing to TAI in 2020, https://www.bipm.org/documents/20126/59466374/10_Table4_TAR20.pdf/0ae3ed2f-f998-9398-fc96-6d12f406f8f6
15. Slyusarev S N et al., in *Metrologiya Vremeni i Prostranstva. Mezhdunarodnyi Simpozium, Mendeleevo, Moskovskaya oblast', Rossiya, 12–14 Sentyabrya 2018* (Metrology of Time and Space. Intern. Symp., Mendeleevo, Moscow Region, Russia, 12–14 September 2018) (Exec. Ed. L A Tokina) (Mendeleevo: VNIIFTRI, 2018)
16. Haroche S et al., in *Laser Spectroscopy IV, Proc. of the Fourth Intern. Conf. on Laser Spectroscopy, June 11–15, 1979, Rottach-Egern, Federal Republic of Germany* (Springer Series in Optical Sciences, Vol. 21, Ed. A L Schawlow) (Berlin: Springer-Verlag, 1979) p. 244
17. Polyakov V, Timofeev Y, Demidov N, in *2021 Joint Conf. of the European Frequency and Time Forum and IEEE Intern. Frequency Control Symp., EFTF/IFCS, Gainesville, FL, USA, 2021* (Piscataway, NJ: IEEE, 2021) p. 1, https://doi.org/10.1109/EFTF/IFCS52194.2021.9604270
18. Basov N G et al. *Sov. Phys. Usp.* **4** 641 (1962); *Usp. Fiz. Nauk* **75** 3 (1961)
19. Ashby N *Living Rev. Relativ.* **6** (1) 1 (2003)
20. Khabarova K *Nature* **602** 391 (2022)
21. Vessot R F C *Phys. Rev. Lett.* **45** 2081 (1980)
22. Delva P et al. *Phys. Rev. Lett.* **121** 231101 (2018)
23. Kovalev Y Y et al., in *2014 XXXIth URSI General Assembly and Scientific Symp., 16–23 August 2014, Beijing, China*
24. Smirov A V et al. *Proc. SPIE* **8442** 1456 (2012)
25. Schiller S et al., arXiv:1206.3765
26. Bakit'ko R V et al. *GLONASS. Modernizatsiya i Perspektivy Razvitiya* (GLONASS. Modernization and Development Prospects) (Moscow: Radiotekhnika, 2020)
27. Mattioni L et al., in *Proc. of the 34th Annual Precise Time and Time Interval Systems and Applications Meeting, December 3–5, 2002, Reston, Virginia*
28. Rochat P et al., in *Proc. of the 2005 IEEE Intern. Frequency Control Symposium and Exposition 26, Vancouver, 2005*
29. Khabarova K et al. *Symmetry* **14** 2213 (2022)
30. Kolachevsky N N et al. *Space* **5** (1) 12 (2018)
31. Fischer M et al. *Phys. Rev. Lett.* **92** 230802 (2004)
32. Bloom B J et al. *Nature* **506** 71 (2014)
33. Ushijima I et al. *Nat. Photon.* **9** 185 (2015)
34. Huang Y et al. *Phys. Rev. Appl.* **17** 034041 (2022)
35. Huntermann N et al. *Phys. Rev. Lett.* **116** 063001 (2016)
36. Khabarova K Yu, Zalivako I V, Kolachevsky N N *Phys. Usp.* **65** 1217 (2022); *Usp. Fiz. Nauk* **192** 1305 (2022)
37. Vishnyakova G A et al. *Phys. Usp.* **59** 168 (2016); *Usp. Fiz. Nauk* **186** 176 (2016)
38. Kalganova E et al. *Phys. Rev. A* **96** 033418 (2017)
39. Takamoto M et al. *Nature* **435** 321 (2005)
40. Tregubov D O et al. *Quantum Electron.* **49** 1028 (2019)
41. Zhang A et al. *Metrologia* **59** 065009 (2022)
42. Ludlow A D et al. *Rev. Mod. Phys.* **87** 637 (2015)
43. Golovizin A *Nat. Commun.* **10** 1724 (2019)
44. Golovizin A et al. *Opt. Express* **29** 36734 (2021)
45. Yudin V I et al. *Phys. Rev. Lett.* **107** 030801 (2011)
46. Golovizin A et al. *Nat. Commun.* **12** 5171 (2021)
47. Kessler T et al. *Nat. Photon.* **6** 687 (2012)
48. Mehlstaeubler T E et al. *Rep. Prog. Phys.* **81** 064401 (2018)
49. Takamoto M et al. *Nat. Photon.* **14** 411 (2020)
50. Huang Y et al. *Phys. Rev. A* **102** 050802 (2020)
51. Dick G J et al., in *Proc. of the 22nd Annual Precise Time and Time Interval Systems and Applications Meeting, December 4–6, 1990, Vienna, Virginia*, p. 487
52. Oelker E et al. *Nat. Photon.* **13** 714 (2019)
53. Takamoto M et al. *C.R. Phys.* **16** 489 (2015)
54. Katori H *Appl. Phys. Express* **14** 072006 (2021)
55. Norcia M A, Thompson J K *Phys. Rev. X* **6** 011025 (2016)
56. Mishin D et al. *Appl. Phys. Express* **14** 112006 (2021)
57. Jallageas A et al. *J. Phys. Conf. Ser.* **723** 012010 (2016)
58. Bothwell T et al. *Nature* **602** 420 (2022)
59. *Nikolai Gennadievich Basov, 100 Let so Dnya Rozhdeniya* (Nikolai Gennadievich Basov, 100 Years since the Birth) (Moscow: Izd. RMP, 2022)
60. King S A et al. *Nature* **611** 43 (2022)
61. Kazakov G A et al. *New J. Phys.* **14** 083019 (2012)
62. Campbell C J et al. *Phys. Rev. Lett.* **108** 120802 (2012)
63. Brasch V et al. *Science* **351** 357 (2016)